prosthesis

MDPI

Article

Comparative Evaluation of Primary Stability in Truncated Cone Implants with Different Macro-Geometries in Low-Density Polyurethane Blocks Simulating Maxillary Sinus Rehabilitations

Luca Comuzzi [1,†], Tea Romasco [2,3,4,*,†], Adriano Piattelli [5,6], Francesco Inchingolo [7], Carlos Fernando Mourão [8] and Natalia Di Pietro [2,3]

1 Independent Researcher, 31020 San Vendemiano, Italy; luca.comuzzi@gmail.com
2 Department of Medical, Oral and Biotechnological Sciences, "G. D'Annunzio" University of Chieti-Pescara, Via dei Vestini 31, 66100 Chieti, Italy; natalia.dipietro@unich.it
3 Center for Advanced Studies and Technology (CAST), "G. D'Annunzio" University of Chieti-Pescara, 66100 Chieti, Italy
4 Division of Dental Research Administration, Tufts University School of Dental Medicine, Boston, MA 02111, USA
5 School of Dentistry, Saint Camillus International University of Health and Medical Sciences, 00131 Rome, Italy; apiattelli51@gmail.com
6 Facultad de Medicina, UCAM Catholic University of Murcia, 30107 Murcia, Spain
7 Department of Interdisciplinary Medicine, University of Bari "Aldo Moro", 70124 Bari, Italy; francesco.inchingolo@uniba.it
8 Department of Clinical and Translational Research, Tufts University School of Dental Medicine, Boston, MA 02111, USA; carlos.mourao@tufts.edu
* Correspondence: tea.romasco@unich.it
† These authors equally contributed to this work.

Citation: Comuzzi, L.; Romasco, T.; Piattelli, A.; Inchingolo, F.; Mourão, C.F.; Di Pietro, N. Comparative Evaluation of Primary Stability in Truncated Cone Implants with Different Macro-Geometries in Low-Density Polyurethane Blocks Simulating Maxillary Sinus Rehabilitations. *Prosthesis* **2024**, *6*, 923–938. https://doi.org/10.3390/prosthesis6040067

Academic Editors: Andrea Scribante, Maurizio Pascadopoli, Simone Gallo and Marco Cicciu

Received: 5 July 2024
Revised: 19 July 2024
Accepted: 6 August 2024
Published: 13 August 2024

Abstract: After tooth loss, particularly in the posterior maxilla, the alveolar ridges undergo bone resorption. Therefore, ensuring the appropriate quantity and quality of alveolar bone is crucial for accurate implant positioning and achieving optimal esthetic and functional results. This study aimed to evaluate biomechanical parameters (insertion torque: IT, removal torque: RT, and implant stability quotient: ISQ) of distinct truncated cone implant designs (Sinus-plant and SLC) on polyurethane blocks simulating type D3 and D4 bone. SLC implants exhibited significantly higher IT, RT, and ISQ values compared to Sinus-plant implants, except in the 10 pounds per cubic foot (PCF) density block with a cortical layer for the IT (24.01 ± 0.91 vs. 23.89 ± 1.66 Ncm). The IT values for SLC implants ranged from 13.95 ± 0.19 Ncm in the lowest density block to 37.94 ± 0.45 Ncm in the highest density block, consistently providing significantly higher primary stability with an ISQ of approximately 70 in the highest density block. Despite lower ISQ in the lowest density block (48.60 ± 0.52 and 48.80 ± 0.42 in buccolingual and mesiodistal directions), it was deemed acceptable considering the inadequate bone densities in the maxillary region. These findings on SLC suggest potential clinical advantages, including reduced procedure duration and costs, improved stability, and the possibility of immediate implant placement following sinus augmentation, thereby streamlining the rehabilitation process.

Keywords: dental implants; maxillary sinus lift; primary stability; polyurethane; truncated cone implants; morse cone connection; healing chambers

1. Introduction

The long-term stability of dental implants hinges upon the establishment of a close and dynamic relationship between the implant surface and the surrounding bone [1]. This relationship is directly influenced by factors such as the initial stability of the implant, the quality and quantity of the bone tissue, the macro- and micro-design of the implant,

surface characteristics, and thread profile. These factors collectively play a pivotal role in facilitating successful implant osseointegration [2,3]. Furthermore, a high level of primary stability enables an immediate loading of the implants, thereby reducing the necessity for multiple surgical interventions and mitigating patient discomfort [4].

Specifically, the ideal ratio between the cortical and trabecular components of bone tissue is crucial for achieving the primary stability of implants. After tooth loss, especially in the posterior maxillary region, the alveolar ridges undergo bone atrophy. Consequently, ensuring the appropriate quantity and quality of alveolar bone is essential for accurate tridimensional implant positioning and optimal esthetic and functional outcomes. A cross-sectional study by Cavalcanti et al. [5] revealed that 41% of sites had a bone height (BH) of less than 5 mm (2.82 $\pm$ 1.57 mm), 40% had a BH between 5 and 8 mm (6.20 $\pm$ 0.79 mm), and 19% had a BH greater than 8 mm (9.42 $\pm$ 1.26 mm). This indicates that in approximately 80% of cases, standard-length implants cannot be placed, suggesting the need for sinus lift surgery for BH of less than 5 mm. Maxillary sinus augmentation procedures are a reliable technique for restoring the correct vertical length for dental implant positioning. When BH is less than or equal to 5 mm, a lateral antrostomy can be performed to access the sinus cavity and perform bone grafting. However, for BH greater than 5 mm, a transcrestal approach can reduce surgical morbidity by avoiding lateral osteotomy and performing a more localized sinus floor elevation, often allowing for immediate dental implant positioning without a second surgical step [6]. The approach to sinus grafting and implant placement may involve either a one-stage or two-stage procedure, depending on the BH. Generally, when the BH falls within the range of 1 to 3 mm, a delayed approach involving a 6-month interval between lateral sinus augmentation and implant insertion is generally recommended. Conversely, a BH measuring $\geq$4–6 mm is generally deemed adequate to support simultaneous sinus elevation and implant placement, ensuring sufficient mechanical stability [7].

In this context, a variety of materials, including autogenous bone grafts and synthetic and animal-derived biomaterials are employed to achieve volume stability [8]. While autogenous bone remains the standard for bone regeneration, collagenated porcine xenografts, whether used alone or in combination with autologous bone, have exhibited notable biocompatibility and osteoconductivity, thereby facilitating new bone formation in sinus augmentation procedures. These findings present collagenated biomaterials as a promising alternative to autologous bone grafts [9–12]. However, the use of short- and ultrashort-length implants has been implemented to reduce rehabilitative times and expenses while demonstrating effective survival rates and primary implant stability [13–16].

Therefore, in extreme maxillary sinus rehabilitation with BH falling between 1 and 3 mm, a comprehensive three-step surgical procedure is conventionally executed. This involves a vestibular sinus lift, subsequent implant insertion following a 6-month period of bone healing, and healing abutment connection 6 months after implant placement. The cumulative time frame for these procedures is approximately one year, with an additional two to three months required to conclude the case [17,18]. On the other hand, retrospective evaluations have demonstrated that simultaneous sinus lift and implant placement with BH ranging from 1 to 3 mm yield a reported 92% cumulative survival rate after 5 years and other reliable outcomes even up to 10 years [19–21]. Similarly, simultaneous transcrestal sinus augmentation and immediate implant placement with a BH of $\geq$4 mm have exhibited high predictability for up to 20 years of follow-up [22]. This simultaneous approach offers diminished clinical morbidity and facilitates a notable reduction in the time necessary for implant restoration, a reduction in the number of surgical phases, and an economic cost-efficiency to rehabilitation.

In order to streamline the process of the majority of extreme maxillary sinus lifts, a new self-condensing truncated cone implant design has been suggested [22–24]. This unique macro-morphology is designed to improve the primary stability of dental implants when placed in the posterior maxilla with limited remaining native bone, aiming to facilitate a one-time surgery, minimize postoperative discomfort, and reduce the overall healing

period to 6–8 months. However, it is crucial to verify the presence of a minimum of 1–3 mm of residual native cortical bone, a vestibular-lingual bone thickness of at least 4.5 mm in the upper premolar or moral regions, and allow for a healing period of 6 months when the bucco-palatal sinus width is less than 12 mm and 9–10 months where the bucco-palatal sinus width equals or exceeds 12 mm before implant loading [25–28].

Misch et al. [29,30] classified bone density into four different categories based on density and the cortical and trabecular microstructure: (i) D1 bone: dense cortical bone with poor/absent trabecular bone (mandibular symphysis); (ii) D2 bone: thick cortical and dense trabecular bone tissue (anterior mandible and anterior maxilla); (iii) D3 bone: thin cortical and less dense trabecular bone (posterior mandible and maxilla); (iv) D4 bone: poor/absent cortical bone with thin trabecular tissue (posterior maxilla); (v) D5 bone: immature bone tissue. Various mathematical and biomechanical models have been developed to substitute human bone for in vitro testing of implant-supported prostheses under loading [31–33]. In the present context, polyurethane is regarded as an isotropic and homogeneous material. It has been designated as a standard prototype by the American Society for Testing and Materials (ASTM) for the examination of force distribution around dental implants at various anatomical sites [34]. The synthetic foam blocks, which mimic oral bone characteristics, are categorized into four groups based on the Misch classification [35,36]: (i) 40 pounds per cubic foot (PCF), corresponding to D1 bone; (ii) 30 PCF, representing D2 bone; (iii) 20 PCF, simulating D3 bone; (iv) and 10 PCF, emulating D4 bone. Numerous in vivo and in vitro investigations have evaluated the primary stability of implants by quantifying the maximum insertion torque (IT) during the process of implant placement [37–41]. In dental implantology, the term IT is used to describe the force required for maximum clockwise movement when removing material. Higher IT values have been found to be beneficial in achieving primary stability by minimizing implant micromotion. Typically, forces of 30 Ncm or higher are commonly employed for implant placement in both healed ridges and fresh extraction sockets, particularly when immediate implant loading is part of the treatment plan. Higher IT values, which are $\geq$50 Ncm, offer the advantage of reducing micromotion without causing damage to the surrounding bone [42,43]. Conversely, removal torque (RT) is clinically defined as the force required to extract the implant from the bone, providing a reliable method for assessing primary stability. Importantly, it indirectly offers insights into the degree of bone-to-implant contact (BIC) [44]. Resonance frequency analysis (RFA) plays a crucial role in evaluating the implant stability quotient (ISQ) following implant placement. This non-invasive technique is invaluable for assessing the risk of implant failure and provides precious information regarding the predictability of dental implant procedures [45].

On these bases, upon conducting a comparison between Sinus-plant (Oralplant Suisse, Mendrisio, Switzerland) and Sinus Lift Concept (SLC, AoN Implants Srl., Grisignano di Zocco, Italy) implants, we aimed to ascertain which truncated cone macro-geometric design performed better on polyurethane blocks artificially simulating type D3 and D4 bone. Specifically, the authors sought to determine the performance in achieving adequate primary stability in the maxillary sinus area. The innovative truncated cone design may have clinical utility by potentially reducing surgery time and costs, minimizing the number of surgical phases, and enhancing the stabilizing effect on the graft and blood clot during sinus rehabilitation. This design could allow for the immediate insertion of the implant after the vestibular sinus lift.

2. Materials and Methods

2.1. Bone Models and Implants

Four different solid rigid polyurethane foams (Sawbones Europe AB, Malmö, Sweden) with the same size (120 mm $\times$ 170 mm $\times$ 40 mm) were used to represent distinct bone densities based on the Misch classification [35,36]:

- 10 PCF polyurethane block (cod. 1522-01) with a density of 0.16 g/cm^3 simulates extremely low-density bone with poor mechanical properties, typically found in the

posterior maxilla or in patients with severe osteoporosis (D4 bone type). This type of bone has sparse or absent cortical bone and thin trabecular tissue;

- 10 PCF polyurethane block laminated with an additional 1 mm, 30 PCF cortical layer (cod. 1522-01 and 1522-102), representing densities of 0.16 g/cm^3 and 0.48 g/cm^3, respectively. This configuration represents a condition where the inner trabecular bone is extremely low-density but has a thin, denser cortical bone layer. This might be seen in osteoporotic patients where the inner bone is compromised, but a thin cortical layer remains intact (D4 bone type with a D2 cortical bone layer);
- 20 PCF polyurethane block (cod. 1522-03), corresponding to 0.32 g/cm^3. It represents low-density bone, often found in the posterior mandible and maxilla or in patients with moderate osteoporosis. This bone type has a thin cortical bone and trabecular bone that is somewhat better in quality compared to D4 bone (D3 bone type);
- 20 PCF polyurethane block and a 30 PCF cortical layer (cod. 1522-03 and 1522-102), representing densities of 0.32 g/cm^3 and 0.48 g/cm^3, respectively. This configuration mimics a condition where the inner trabecular bone is of moderate density, with a preserved, denser cortical bone layer. This might be found in areas of localized low bone density where cortical integrity is maintained, offering better overall bone quality than the 10 PCF block with a 30 PCF layer (D3 bone type with a D2 cortical bone layer).

The artificial bone blocks utilized in this study are depicted in Figure 1.

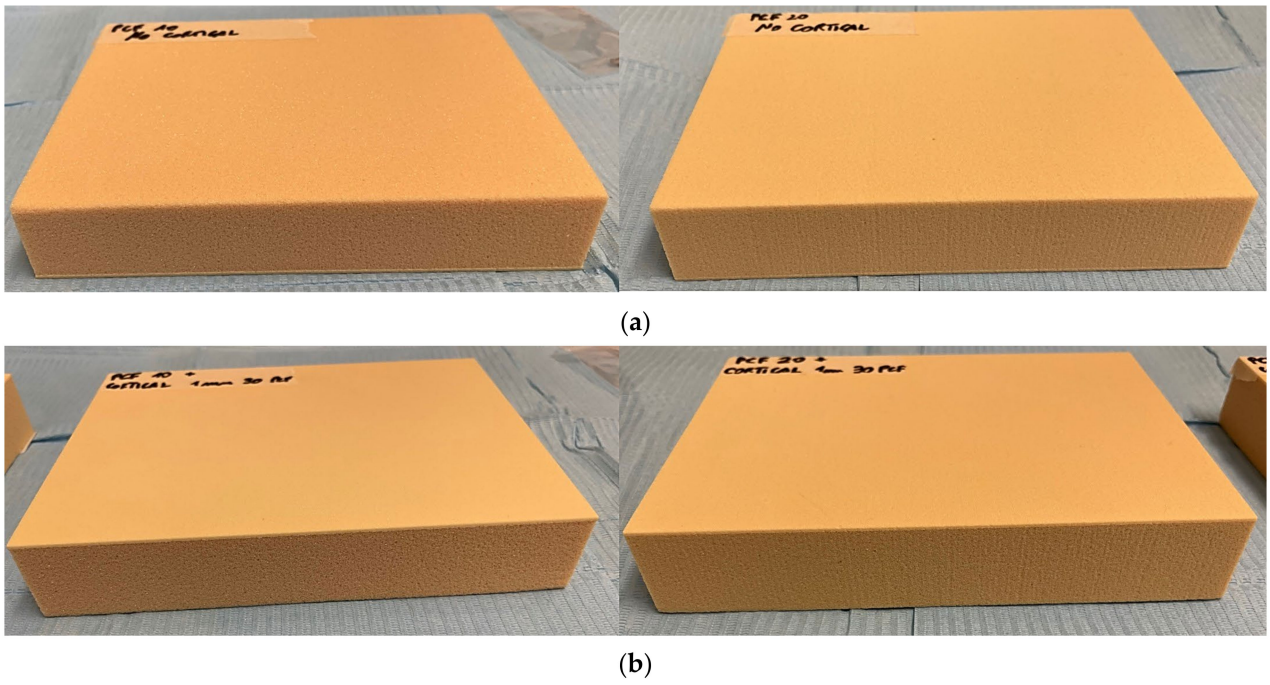

(**a**)

(**b**)

Figure 1. Solid rigid polyurethane foams used in the present study. (**a**) 20 and 10 pounds per cubic foot (PCF) density blocks without the cortical layer; (**b**) 20 and 10 PCF density blocks with the additional 1 mm, 30 PCF cortical layer.

All tested implants were inserted into 20 and 10 PCF density artificial bone blocks with or without a 1 mm, 30 PCF cortical layer. Specifically, two distinct truncated cone implant designs have been considered: Sinus-plant (Oralplant Suisse, Mendrisio, Switzerland) and SLC (AoN Implants Srl., Grisignano di Zocco, Italy), with diameters of 4.5 and 4.2 mm, respectively, and lengths of 10 mm. Although the dental implants possessed slightly different diameters, we selected the most closely matched dimensions for comparison, as the manufacturers did not produce implants with identical diameters. The Sinus-plant implants feature a straight head shape and a dome apex shape devoid of grooves, able to maintain the integrity of the Schneiderian membrane and facilitate a controlled insertion pressure. The V-shaped threads, characterized by a 0.4 mm pitch profile, mitigate stress

while fostering gradual bone expansion and osseodensification. Furthermore, these implants boasted a Titanium Pull Spray Superficial (TPSS) surface, achieved through precise treatment with 0.5-micron aluminum oxide tips, resulting in the formation of rounded and porous surface microcavities [24]. On the other hand, the technical features of SLC implants encompass a machined surface and a lapped apex to ensure controlled and atraumatic implant penetration, tailored explicitly for maxillary sinus lifts. A progressive and expansive thread pitch from the apex to the platform also contributes to progressive bone expansion. The self-tapping/self-drilling V-shaped threads exhibit a 1.17 mm pitch profile and an 11° thread angle, while helical drains along the body facilitate the collection and removal of bone chips during implant insertion. This design minimizes debris accumulation at the site, reducing the risk of interference with primary stability and proper implant osseointegration. Furthermore, it aids in collecting bone chips and defusing blood, fostering an osteopromotive environment and enhancing bone integration.

Both grade IV titanium implants are equipped with an internal Morse cone connection and a switching platform, which effectively minimize marginal bone level changes and provide superior sealing to reduce bacterial colonization in comparison to alternative connections (Figure 2) [46,47].

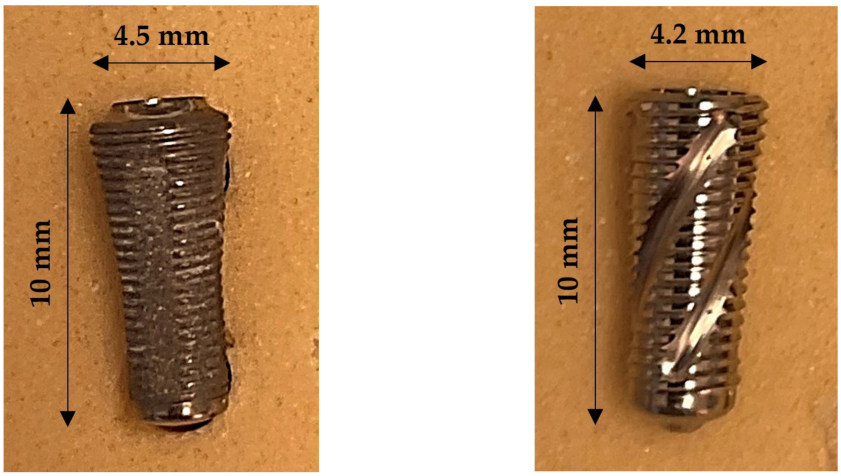

(**a**) (**b**)

Figure 2. Representative images of the implants analyzed in this study. (**a**) Sinus-plant implant design; (**b**) Sinus Lift Concept (SLC) implant design.

2.2. Drilling Protocol and Study Design

The study was performed by a single operator (LC), who standardized the protocol for the placement of implants in different blocks, regardless of the implant type. The drilling sequence involved a lance drill with a diameter of 2 mm, followed by a 2.2 mm drill and then a 3.2 mm drill (AoN Implants Srl., Grisignano di Zocco, Italy) using a surgical implant motor (Chiropro, Bien Air, Bienne, Switzerland) set at 100 rpm (Figure 3).

The final implant placement was achieved at the crest level, using a speed of 30 rpm and a predetermined maximum torque of 45 Ncm. IT and RT values were recorded at the final millimeter of the implant site using a calibrated torque meter (Figure 4).

Additionally, the RFA was measured using a dedicated device (Smartpeg n.78) and a frequency response analyzer (Osstell Beacon, Ostell Inc., Göteborg, Sweden), capturing the ISQ in two different orientations at 90 degrees (mesiodistal: MD and buccolingual: BL) (Figure 5).

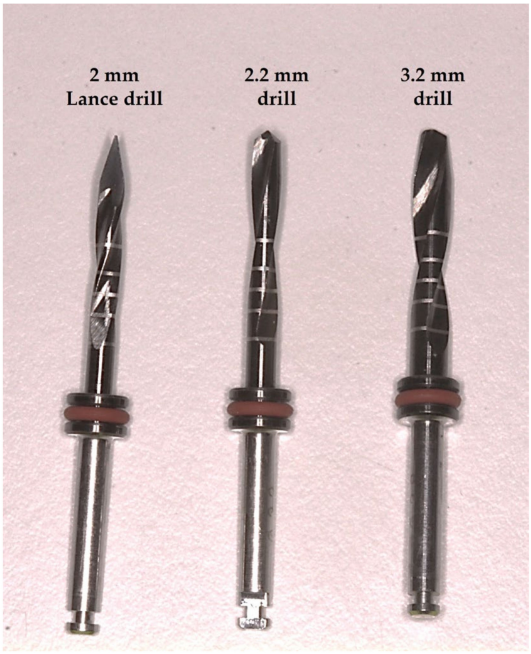

Figure 3. Details of drills used for both implants in this in vitro study.

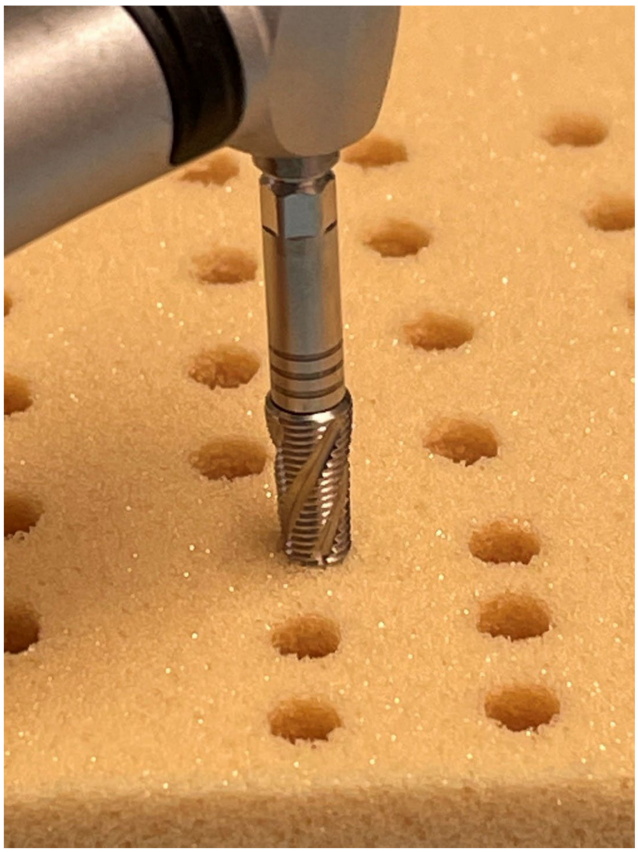

Figure 4. Representative picture of the SLC implant insertion into a block with 10 PCF density without cortical layer.

Figure 5. Representative picture of the Sinus-plant implant stability quotient (ISQ) measurements in the buccolingual (BL) and mesiodistal (MD) directions, after insertion into a 20 PCF density block with a cortical layer. A combined total of 104 osteotomies were conducted, with 13 performed for each type of implant across the different polyurethane foam models (52 total osteotomies for each implant type). Consequently, 26 drilling sites were established for each block, as illustrated in Figure 6.

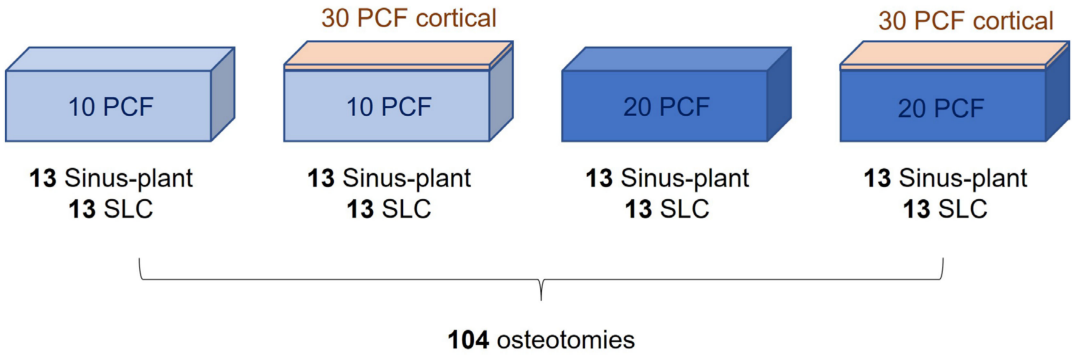

Figure 6. Scheme of the study design.

2.3. Data Analysis

The G*Power 3.1.9.7 program (Heinrich Heine Universität Düsseldorf, Düsseldorf, Germany) was used for the sample size calculation and power analysis. This was conducted within the F tests family and an analysis of variance (ANOVA): fixed effects, special, main effects, and interactions statistical test (effect size: 0.4; α err: 0.05; power (1-β): 0.8; numerator df: 7; number of groups: 8). The dependent variables considered for the sample size calculation were the IT, RT, and BL and MD RFA measurements, while the independent variables were the implant type, the bone density, and the presence or absence of a cortical layer. The minimum sample size required for statistical significance was determined to be 97 implants, with 12 samples per group.

Furthermore, the study employed a 2 $\times$ 2 $\times$ 2 factorial design, incorporating the factors "implant type" (SLC and Sinus-plant implants), "artificial bone density" (10 and 20 PCF), and "cortical layer" (presence or absence). This design was analyzed using a three-way ANOVA model and Tukey's post hoc test. Descriptive statistics were presented as means and corresponding standard deviations (SD). Statistical significance was determined by considering *p*-values equal to or less than 0.05. All statistical analyses were conducted using the GraphPad 9.0 software package (Prism, San Diego, CA, USA).

3. Results

3.1. Insertion Torque (IT)

After the insertion of implants, the maximum IT value was recorded for each implant, encompassing all polyurethane bone densities. Figure 7 depicts the average IT value comparisons, while Table S1 (Supplementary Material S1) provides a comprehensive overview of the significance of each intergroup comparison.

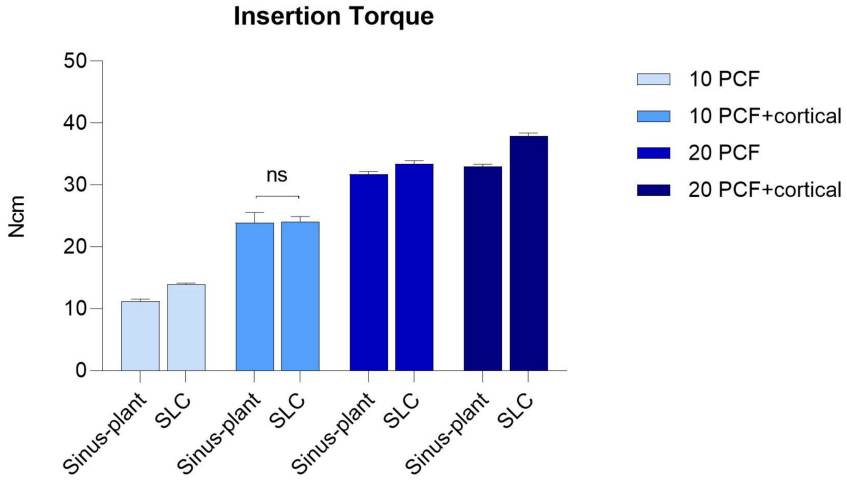

Figure 7. Mean insertion torque (IT) values recorded for Sinus-plant and SLC implants across various artificial bone densities. ns: not significant.

It was observed that the IT exhibited a direct correlation with the polyurethane density, with the lowest IT values recorded in the 10 PCF density block without a cortical layer (Sinus-plant: 11.23 ± 0.35 Ncm, SLC: 13.95 ± 0.19 Ncm), and the highest values in the 20 PCF density block with the cortical sheet for both implant types (Sinus-plant: 33.03 ± 0.34 Ncm, SLC: 37.94 ± 0.45 Ncm). Furthermore, the presence of a cortical layer notably influenced the IT, resulting in significantly higher values with implants inserted in the 10 and 20 PCF blocks with the cortical sheet compared to the corresponding block without cortical sheet (Sinus-plant: $p < 0.0001$ and $p < 0.01$, respectively; SLC: $p < 0.0001$ and $p < 0.0001$, respectively).

Overall, all multiple comparisons among polyurethane densities yielded statistically significant differences with a $p < 0.0001$, with the exception of the Sinus-plant implants comparing the 20 PCF block with the cortical layer to the 20 PCF density block without it, which exhibited a $p < 0.01$.

Additionally, even all multiple comparisons between implant types inserted in the same artificial bone density yielded statistically significant differences, except for the 10 PCF density block with the cortical layer (Sinus-plant: 23.89 ± 1.66 Ncm, SLC: 24.01 ± 0.91 Ncm). Specifically, the SLC implants exhibited higher IT values in every experimental condition.

3.2. Removal Torque (RT)

From Figure 8, it can be observed that the RT values for both Sinus-plant and SLC implants exhibited similar trends to the IT ones across all polyurethane densities, except for the 10 PCF density block with the cortical layer, in which Sinus-plant implants displayed significantly higher results (Sinus-plant: 22.17 ± 1.19 Ncm, SLC: 21.17 ± 0.38 Ncm, $p < 0.01$).

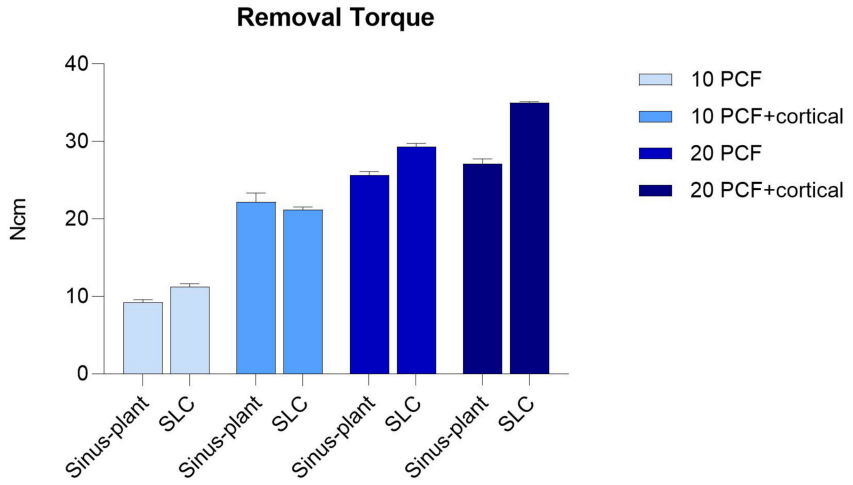

Figure 8. Mean removal torque (RT) values recorded for Sinus-plant and SLC implants across various artificial bone densities.

The lowest RT values were recorded in the lowest density block (Sinus-plant: 9.22 ± 0.37 Ncm, SLC: 11.20 ± 0.46 Ncm), while the highest ones were observed in the 20 PCF density block with the cortical layer (Sinus-plant: 27.14 ± 0.63 Ncm, SLC: 35.01 ± 0.14 Ncm). Similar to IT measurements, all multiple comparisons among polyurethane densities and between the implant types within each density demonstrated statistically significant differences with a $p < 0.0001$. The SLC implants consistently exhibited higher values, except in the 10 PCF density block with the cortical layer.

Moreover, it was noted that the RT values did not notably differ from the IT values. Although the RT values were lower than the corresponding IT values in the same density block, the differences ranged from approximately 2–3 Ncm for both implants inserted in the 10 PCF density block to 3–6 Ncm in the 20 PCF density block with the cortical layer.

The multicomparison results and corresponding *p*-values can be found in Table S2 of the Supplementary Materials (S2).

3.3. Resonance Frequency Analysis (RFA)

ISQ values were obtained from two distinct orientations for each implant when measuring implant stability. Tables S3 and S4 (Supplementary Materials S3 and S4) offer an analysis of the statistical significance for each comparison between groups.

Similar to the IT and RT, the RFA was directly proportional to the density of the artificial bone. The implants demonstrated the lowest ISQ values within the 10 PCF density block, with the Sinus-plant registering 45.80 ± 0.78 ISQ in the BL direction and 46.20 ± 0.79 ISQ in the MD direction, and the SLC showing 48.60 ± 0.52 ISQ in the BL direction and 48.80 ± 0.42 ISQ in the MD direction. Conversely, the 20 PCF density block with the cortical sheet exhibited the highest ISQ values, with the Sinus-plant recording 62.71 ± 0.48 ISQ in the BL direction and 62.51 ± 0.53 ISQ in the MD direction and the SLC registering 69.41 ± 0.52 ISQ in the BL direction and 69.50 ± 0.52 ISQ in the MD direction.

ISQ values of 70 or higher represent high stability, values between 60 and 69 represent medium stability, and values below 60 represent low stability [48]. A high primary stability was achieved only with SLC implants in the highest-density block with ISQ values of approximately 70 in both directions (BL: 69.40 ± 0.52 ISQ, MD: 69.51 ± 0.53 ISQ). The primary stability was considered medium with both implants in all the other experimental conditions, except for the lowest density block and Sinus-plant implants in the 10 PCF density block with a cortical layer (BL: 56.32 ± 0.68, MD: 56.40 ± 0.07 ISQ). In these cases, the ISQ was low.

Notably, statistically significant differences with a $p < 0.0001$ were evident for both implants across all multiple comparisons within the experimental conditions (Figure 9).

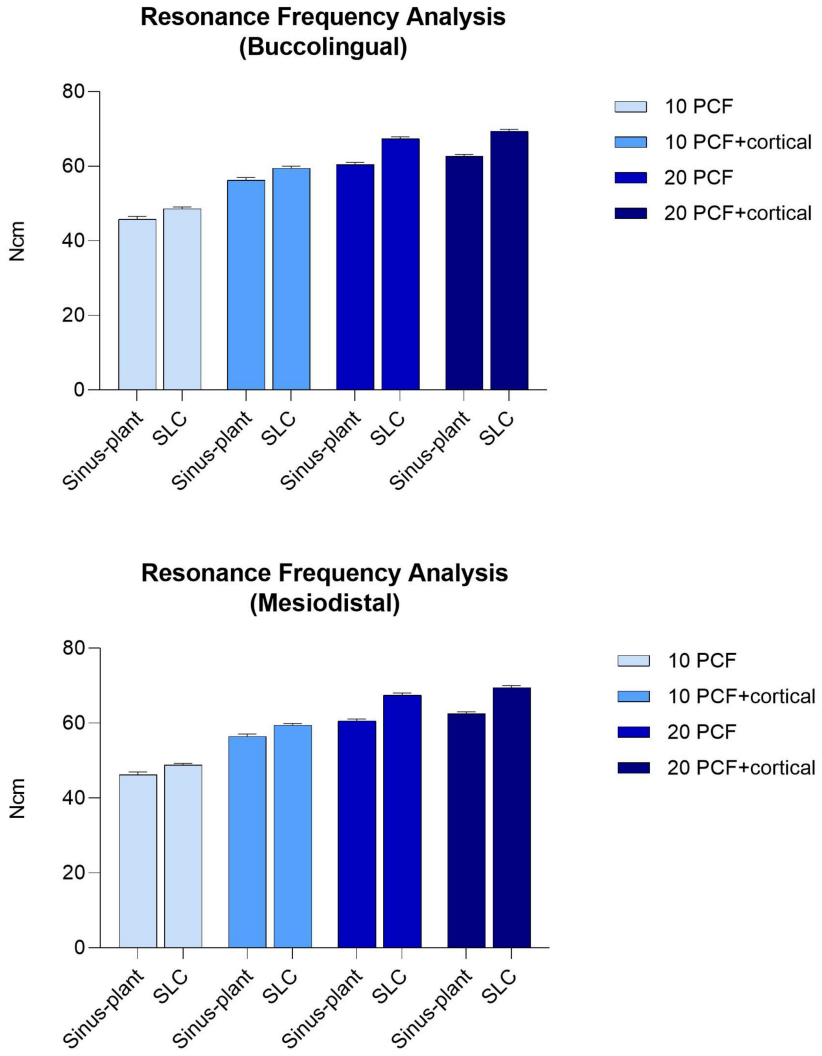

Figure 9. Mean ISQ values recorded in the BL and MD orientations for Sinus-plant and SLC implants across various artificial bone densities.

4. Discussion

The primary objective of this study was to assess and compare the biomechanical parameters (IT, RT, and RFA) of distinct truncated cone implant macro-morphologies (Sinus-plant and SLC) on polyurethane blocks artificially simulating type D3 and D4 bone. The potential clinical impact of identifying the most effective truncated cone implant design includes the reduction in procedure duration, costs, and invasiveness associated with extreme maxillary sinus rehabilitations. Furthermore, it may enable immediate implant placement following sinus augmentation, allowing for a one-stage rehabilitation period of 6–8 months.

Following the insertion of implants, the highest recorded values for IT, RT, and RFA were noted for each implant across different polyurethane bone densities. It is noteworthy that these parameters were observed to be influenced by both the artificial bone density and the presence of a cortical sheet. Specifically, the lowest values were consistently identified within the 10 PCF density block, while the highest values within the 20 PCF block featuring a cortical layer. This trend was reported for both types of implants across all cases, with the addition of a cortical layer resulting in significantly higher values compared to the corresponding block lacking a cortical layer. These findings are in alignment with the existing literature, which underscores that a reduced primary stability is evidenced in low-density bone and emphasizes that the thickness of the cortical layers significantly

impacts the initial stability of implants [16,41,49–52]. The IT, RT, and ISQ are all indirectly associated with the primary stability of implants. The IT method has demonstrated a higher predictability of osseointegration and has been shown to be proportionally correlated with implant primary stability by minimizing implant micromotion [42]. Furthermore, the ISQ quantitative assessment, in conjunction with the RT technique, is considered an indirect indicator of BIC [44,45]. The poor primary stability experienced in low-density bone may result in micro-movements of the implant, hindering the process of osseointegration. Consequently, this can lead to a longer healing period prior to loading and an elevated risk of early implant failure. Considering that the ISQ encompasses a spectrum from 0 to 100, with a threshold of 47 denoting favorable implant stability [53,54], the current assessment revealed that an optimal level of primary stability was exclusively attained with SLC implants within the highest density block, yielding ISQ values around 70 in both directions (BL: 69.40 $\pm$ 0.52 ISQ, MD: 69.51 $\pm$ 0.53 ISQ). On the contrary, low primary stability has been observed in the 10 PCF density block for both implants (Sinus-plant: 45.80 $\pm$ 0.78 ISQ in the BL direction and 46.20 $\pm$ 0.79 ISQ in the MD direction; SLC: 48.60 $\pm$ 0.52 ISQ in the BL direction and 48.80 $\pm$ 0.42 ISQ in the MD direction), as per Sennerby and Meredith [48]. Nevertheless, this was deemed acceptable when accounting for the insufficient bone densities in the maxillary region. In summary, SLC implants always exhibited significantly superior RFA as compared to Sinus-plant implants across all experimental conditions. Similarly, SLC implants demonstrated significantly higher IT values compared to Sinus-plant implants across all polyurethane densities, with the exception of the 10 PCF density block with the cortical layer (Sinus-plant: 23.89 $\pm$ 1.66 Ncm, SLC: 24.01 $\pm$ 0.91 Ncm). The IT values for this implant design ranged from 13.95 $\pm$ 0.19 Ncm in the lowest density block to 37.94 $\pm$ 0.45 Ncm in the highest density block, allowing for subsequent superior primary stability across all artificial bone densities. Furthermore, it was noteworthy that the lower the polyurethane density, the more pronounced the stabilizing effect of the cortical layer. Indeed, in the 10 PCF density block, the cortical layer increased the IT by approximately 10–13 Ncm for both implants, whereas in the 20 PCF density block, the increase was approximately 2–5 Ncm for both. It should be also highlighted that the RT values displayed similar trends to the IT values across all polyurethane blocks, with only slight variations between the two parameters, ranging from 2–3 Ncm for both implants inserted in the 10 PCF density block to 3–6 Ncm in the 20 PCF density block with the cortical layer. However, in the 10 PCF density block with the cortical sheet, Sinus-plant implants exhibited significantly higher RT values compared to SLC implants (Sinus-plant: 22.17 $\pm$ 1.19 Ncm, SLC: 21.17 $\pm$ 0.38 Ncm, $p < 0.01$). Similar to the IT measurements, all comparisons among polyurethane densities and between implant types within each density yielded statistically significant differences ($p < 0.0001$).

On these bases, it is crucial to emphasize the significance of bone quality, implant design, and thread configuration as vital determinants impacting the primary stability of dental implants [2,16,38,55,56]. While previous studies have presented differing outcomes regarding the impact of these factors on primary stability, it appears that implant length and diameter mainly affect the ISQ in low-density bone, with shorter and narrower implants yielding significantly lower results [41,57]. Furthermore, studies investigating the influence of implant and thread shape on primary stability have demonstrated that conical or truncated-shaped implants exhibit higher ISQ values and superior clinical outcomes compared to cylindrical ones in low-density bone. Additionally, it was found that implants without apical modifications or innovative designs, such as the Blossom cutting design of the threads, displayed the highest ISQ in comparison to cutting flute-shaped implants in low-density bone [56,58,59].

The truncated cone shape of implants offers distinct advantages, particularly in low-density bone and various clinical scenarios, such as the posterior maxilla, where the cortical compartment is reduced, and the cancellous/medullary spaces are wider [22–24], and maxillary sinus pneumatization in posterior edentulous areas within bone augmentation procedures [60]. Specifically, these implants are characterized by a cylindrical shape

that extends from the apex to a few millimeters towards the coronal region, where it undergoes a transition into a tapered form. The design under consideration facilitated the stabilization of implants by enabling progressive fixation into the polyurethane material, ultimately achieving maximum torque near the platform engagement. Notably, while both implants exhibited similar mechanical friction characteristics, the SLC implant may offer superior clinical advantages. Firstly, the SLC's smaller final hole diameter enhances its versatility, especially in narrow bone platform situations. Additionally, the specific self-condensing truncated cone shape of this implant supports progressive bone expansion without inducing stress [16]. The threads on the SLC implant allowed controlled and gradual advancement, minimizing bone stress, while the less pronounced thread design of the Sinus-plant impeded its progression, favoring external chip expulsion and partially stripping the hole's threading. In contrast, the SLC's advanced thread design, with three bone decompression niches, accumulated polyurethane debris into the niches, resembling clinical conditions where bone chips promote osseointegration, thereby enabling constant and progressive implant advancement, keeping the osteotomy clean [61–63]. The 1-mm under-preparation provided by the final drill for the SLC appeared optimal across all bone density conditions. Furthermore, the rounded tip shape of the SLC allowed advancement in the osteotomy hole despite not being designed for that purpose. It was intended to maintain the integrity of the Schneiderian membrane and facilitate controlled insertion pressure. Moreover, the self-condensing nature of this screw eliminates the need for the osteotome technique for implant bed preparation.

The sinus augmentation procedures are generally focused on the amount of remaining vertical bone tissue, with either a two-stage or single-stage surgery [6,7]. Achieving successful primary stability with 1–3 mm of residual bone can lead to a substantial reduction in the recovery period, fewer surgical interventions, and cost-effective procedures [64]. This implant macro-morphology may allow for combined sinus lift, implant placement, and insertion of the healing screw in a single surgery over a period of 6–8 months. However, condensing an extreme lateral sinus augmentation into a single procedure is recommended when utilizing the characteristics design of SLC only with the presence of a minimum of 1–3 mm of residual native cortical bone and a BL bone thickness of at least 4.5 mm in the upper premolar or moral regions. Prior to implant loading, a healing period of 6 months is recommended if the bucco-palatal sinus width is less than 12 mm, whereas 9–10 months are advisable if the width equals or exceeds 12 mm [25–28]. However, it is imperative to exercise caution and refrain from employing this technique in instances of any poorly healed bone or post-extraction sockets lacking a well-represented septum, particularly in areas outside the upper posterior maxilla and when it is unnecessary, such as when 8–10 mm of bone is present.

The outcomes of this study are subject to certain limitations given the use of an artificial bone model, making it evident that the results may not be directly applied to clinical scenarios. It is crucial to recognize that while polyurethane foam blocks serve as a reliable in vitro model for implant research as alternatives to cadaver or animal bones due to their consistent and reproducible testing properties, they are unable to completely replicate the intricate features of natural bone [65,66]. Various considerations should be taken into account for comprehensive data analysis, including the absence of individual human variability, natural bone response, and the complex microenvironment of healthy or pathological bone. Furthermore, factors related to surgical technique should be considered to facilitate a more accurate interpretation of these results. Consequently, it is imperative to validate these findings through animal and clinical studies for their future utilization and implementation. To enhance the use of polyurethane blocks as a human bone model for studying implant behavior, conducting biomechanical assessments using finite element analysis (FEA) studies could be contemplated [67–69]. In conclusion, despite the limitations of an in vitro study using non-human bone tissue, the authors suggest that these preliminary results may provide valuable insights into the biomechanical

behavior of these implants, aiming to assist clinicians in enhancing their surgical sinus rehabilitation planning.

5. Conclusions

Upon comparative analysis of the truncated cone Sinus-plant (Oralplant Suisse, Mendrisio, Switzerland) and SLC (AoN Implants Srl., Grisignano di Zocco, Italy) implants, the superior performance of the innovative SLC design in achieving primary stability within polyurethane blocks simulating type D3 or D4 bone in the maxillary sinus region offers potential clinical advantages. Specifically, they include the reduction of surgical duration and costs, the streamlining of surgical phases, and the enhancement of graft and blood clot stabilization during sinus rehabilitation. Notably, this design could potentially facilitate immediate implant insertion after an extreme vestibular sinus augmentation procedure. Furthermore, despite the limitations of this study, further validations are recommended to confirm these preliminary findings and enhance their applicability in clinical practice.

Supplementary Materials: The following supporting information can be downloaded at: https://www.mdpi.com/article/10.3390/prosthesis6040067/s1. Table S1: *p*-values and confidence intervals (CI) regarding the multiple insertion torque (IT) values comparisons across the experimental groups; Table S2: *p*-values and CI regarding the multiple removal torque (RT) value comparisons across the experimental groups; Table S3: *p*-values and CI regarding the multiple implant stability quotient (ISQ) value comparisons across the experimental groups in the buccolingual (BL) direction; Table S4: *p*-values and CI regarding the multiple ISQ value comparisons across the experimental groups in the mesiodistal (MD) direction.

Author Contributions: Conceptualization, L.C., C.F.M., A.P. and N.D.P.; methodology, L.C. and F.I.; software, L.C. and T.R.; validation, A.P., C.F.M. and N.D.P.; formal analysis, T.R. and N.D.P.; investigation, L.C., T.R. and F.I.; resources, L.C. and N.D.P.; data curation, T.R. and N.D.P.; writing—original draft preparation, L.C. and T.R.; writing—review and editing, T.R.; visualization, T.R. and N.D.P.; supervision, A.P. and N.D.P.; project administration, L.C. and N.D.P.; funding acquisition, L.C. All authors have read and agreed to the published version of the manuscript.

Funding: This research received no external funding.

Institutional Review Board Statement: Not applicable.

Informed Consent Statement: Not applicable.

Data Availability Statement: The original contributions presented in the study are included in the article/Supplementary Materials, further inquiries can be directed to the corresponding author.

Acknowledgments: AoN Implants S.r.l. Company, Grisignano di Zocco, Vicenza, Italy, provided the implants at no cost, and this is gratefully acknowledged.

Conflicts of Interest: The authors declare no conflicts of interest.

References

1. Albrektsson, T.; Albrektsson, B. Osseointegration of bone implants: A review of an alternative mode of fixation. *Acta Orthop. Scand.* **1987**, *5*, 567–577. [CrossRef]
2. Javed, F.; Ahmed, H.B.; Crespi, R.; Romanos, G.E. Role of primary stability for successful osseointegration of dental implants: Factors of influence and evaluation. *Interv. Med. Appl. Sci.* **2013**, *5*, 162–167. [CrossRef]
3. Heimes, D.; Becker, P.; Pabst, A.; Smeets, R.; Kraus, A.; Hartmann, A.; Sagheb, K.; Kämmerer, P.W. How does dental implant macrogeometry affect primary implant stability? A narrative review. *Int. J. Implant. Dent.* **2023**, *9*, 20. [CrossRef] [PubMed]
4. Tettamanti, L.; Andrisani, C.; Bassi, M.A.; Vinci, R.; Silvestre-Rangil, J.; Tagliabue, A. Immediate loading implants: Review of the critical aspects. *Oral Implantol.* **2017**, *10*, 129–139. [CrossRef]
5. Cavalcanti, M.C.; Guirado, T.E.; Sapata, V.M.; Costa, C.; Pannuti, C.M.; Jung, R.E.; César Neto, J.B. Maxillary sinus floor pneumatization and alveolar ridge resorption after tooth loss: A cross-sectional study. *Braz. Oral Res.* **2018**, *32*, e64. [CrossRef]
6. Misch, C.E. Maxillary sinus augmentation for endosteal implants: Organized alternative treatment plans. *Int. J. Oral Implantol.* **1987**, *4*, 49–58. [PubMed]
7. Jensen, O.T.; Shulman, L.B.; Block, M.S.; Iacono, V.J. Report of the Sinus Consensus Conference of 1996. *Int. J. Oral Maxillofac. Implants* **1998**, *13*, 11–45. [PubMed]

8. Pesce, P.; Menini, M.; Canullo, L.; Khijmatgar, S.; Modenese, L.; Gallifante, G.; Del Fabbro, M. Radiographic and Histomorphometric Evaluation of Biomaterials Used for Lateral Sinus Augmentation: A Systematic Review on the Effect of Residual Bone Height and Vertical Graft Size on New Bone Formation and Graft Shrinkage. *J. Clin. Med.* **2021**, *10*, 4996. [CrossRef]
9. Correia, F.; Gouveia, S.; Felino, A.C.; Faria-Almeida, R.; Pozza, D.H. Maxillary Sinus Augmentation with Xenogenic Collagen-Retained Heterologous Cortico-Cancellous Bone: A 3-Year Follow-Up Randomized Controlled Trial. *Dent. J.* **2024**, *12*, 33. [CrossRef]
10. Scarano, A.; Piattelli, A.; Perrotti, V.; Manzon, L.; Iezzi, G. Maxillary sinus augmentation in humans using cortical porcine bone: A histological and histomorphometrical evaluation after 4 and 6 months. *Clin. Implant Dent. Relat. Res.* **2011**, *13*, 13–18. [CrossRef]
11. Cassetta, M.; Perrotti, V.; Calasso, S.; Piattelli, A.; Sinjari, B.; Iezzi, G. Bone formation in sinus augmentation procedures using autologous bone, porcine bone, and a 50:50 mixture: A human clinical and histological evaluation at 2 months. *Clin. Oral. Implants Res.* **2015**, *26*, 1180–1184. [CrossRef]
12. Romasco, T.; Tumedei, M.; Inchingolo, F.; Pignatelli, P.; Montesani, L.; Iezzi, G.; Petrini, M.; Piattelli, A.; Di Pietro, N. A Narrative Review on the Effectiveness of Bone Regeneration Procedures with OsteoBiol® Collagenated Porcine Grafts: The Translational Research Experience over 20 Years. *J. Funct. Biomater.* **2022**, *13*, 121. [CrossRef] [PubMed]
13. Yu, X.; Xu, R.; Zhang, Z.; Yang, Y.; Deng, F. A meta-analysis indicating extra-short implants ($\leq$6 mm) as an alternative to longer implants ($\geq$8 mm) with bone augmentation. *Sci. Rep.* **2021**, *11*, 8152. [CrossRef] [PubMed]
14. Lombardo, G.; Signoriello, A.; Marincola, M.; Nocini, P.F. Assessment of Peri-Implant Soft Tissues Conditions around Short and Ultra-Short Implant-Supported Single Crowns: A 3-Year Retrospective Study on Periodontally Healthy Patients and Patients with a History of Periodontal Disease. *Int. J. Environ. Res. Public Health* **2020**, *17*, 9354. [CrossRef]
15. Pistilli, R.; Zucchelli, G.; Barausse, C.; Bonifazi, L.; Karaban, M.; Gasparro, R.; Felice, P. Minimally Invasive Fixed Rehabilitation of an Extremely Atrophic Posterior Mandible Using 4-mm Ultrashort Implants: A Case Report with a 7-Year Follow-up. *Int. J. Periodontics Restor. Dent.* **2020**, *40*, e235–e240. [CrossRef]
16. Comuzzi, L.; Tumedei, M.; Romasco, T.; Petrini, M.; Afrashtehfar, K.I.; Inchingolo, F.; Piattelli, A.; Di Pietro, N. Insertion Torque, Removal Torque, and Resonance Frequency Analysis Values of Ultrashort, Short, and Standard Dental Implants: An In Vitro Study on Polyurethane Foam Sheets. *J. Funct. Biomater.* **2023**, *14*, 10. [CrossRef]
17. Lyu, M.; Xu, D.; Zhang, X.; Yuan, Q. Maxillary sinus floor augmentation: A review of current evidence on anatomical factors and a decision tree. *Int. J. Oral Sci.* **2023**, *15*, 41. [CrossRef]
18. Krasny, K.; Krasny, M.; Kamiński, A. Two-stage closed sinus lift: A new surgical technique for maxillary sinus floor augmentation. *Cell Tissue Bank.* **2015**, *16*, 579–585. [CrossRef]
19. Scarano, A.; Piattelli, A.; Assenza, B.; Quaranta, A.; Perrotti, V.; Piattelli, M.; Iezzi, G. Porcine bone used in sinus augmentation procedures: A 5-year retrospective clinical evaluation. *J. Oral Maxillofac. Surg.* **2010**, *68*, 1869–1873. [CrossRef]
20. Virnik, S.; Cueni, L.; Kloss-Brandstätter, A. Is one-stage lateral sinus lift and implantation safe in severely atrophic maxillae? Results of a comparative pilot study. *Int. J. Implant Dent.* **2023**, *9*, 6. [CrossRef]
21. Pistilli, R.; Canullo, L.; Pesce, P.; Pistilli, V.; Caponio, V.C.A.; Sbricoli, L. Guided implant surgery and sinus lift in severely resorbed maxillae: A retrospective clinical study with up to 10 years of follow-up. *J. Dent.* **2022**, *121*, 104137. [CrossRef]
22. Comuzzi, L.; Tumedei, M.; Piattelli, A.; Tartaglia, G.; Del Fabbro, M. Radiographic Analysis of Graft Dimensional Changes in Transcrestal Maxillary Sinus Augmentation: A Retrospective Study. *Materials* **2022**, *15*, 2964. [CrossRef]
23. Comuzzi, L.; Tumedei, M.; Petrini, M.; Romasco, T.; Lorusso, F.; De Angelis, F.; Piattelli, A.; Tatullo, M.; Di Pietro, N. Clinical and Radiological Evaluation of a Self-Condensing Bone Implant in One-Stage Sinus Augmentation: A 3-Year Follow-up Retrospective Study. *Int. J. Environ. Res. Public Health* **2023**, *20*, 2583. [CrossRef] [PubMed]
24. Comuzzi, L.; Iezzi, G.; Lucchese, A.; Di Pietro, N.; Balice, P.; D'Arcangelo, C.; Piattelli, A.; Tumedei, M. Mechanical Behaviour and Primary Stability of a Self-Condensing Implant: A Laboratory Critical Simulation of a Severe Maxillary Atrophy on Polyurethane Lamina. *Appl. Sci.* **2022**, *12*, 966. [CrossRef]
25. Avila, G.; Wang, H.L.; Galindo-Moreno, P.; Misch, C.E.; Bagramian, R.A.; Rudek, I.; Benavides, E.; Moreno-Riestra, I.; Braun, T.; Neiva, R. The influence of the bucco-palatal distance on sinus augmentation outcomes. *J. Periodontol.* **2010**, *81*, 1041–1050. [CrossRef]
26. Šimůnek, A.; Kopecká, D.; Brázda, T.; Somanathan, R.V. Is lateral sinus lift an effective and safe technique? Contemplations after the performance of one thousand surgeries. *Implantol. J.* **2007**, *5*, 1–5.
27. Stacchi, C.; Lombardi, T.; Ottonelli, R.; Berton, F.; Perinetti, G.; Traini, T. New bone formation after transcrestal sinus floor elevation was influenced by sinus cavity dimensions: A prospective histologic and histomorphometric study. *Clin. Oral Implants Res.* **2018**, *29*, 465–479. [CrossRef] [PubMed]
28. Stacchi, C.; Spinato, S.; Lombardi, T.; Bernardello, F.; Bertoldi, C.; Zaffe, D.; Nevins, M. Minimally Invasive Management of Implant-Supported Rehabilitation in the Posterior Maxilla, Part I. Sinus Floor Elevation: Biologic Principles and Materials. *Int. J. Periodontics Restor. Dent.* **2020**, *40*, e85–e93. [CrossRef] [PubMed]
29. Misch, C.E.; Judy, K.W. Classification of partially edentulous arches for implant dentistry. *Int. J. Oral Implantol.* **1987**, *4*, 7–13.
30. Misch, C.E. Bone density: A key determinant for clinical success. *Contemp. Implant Dent.* **1999**, *8*, 109–118.
31. Tabrizi, A.; Rizzo, P.; Ochs, M.W. Electromechanical impedance method to assess dental implant stability. *Smart Mater. Struct.* **2012**, *21*, 115022. [CrossRef]

32. Jar, C.; Archibald, A.; Gibson, M.; Westover, L. An analytical model to measure dental implant stability with the Advanced System for Implant Stability Testing (ASIST). *J. Mech. Behav. Biomed. Mater.* **2024**, *150*, 106238. [CrossRef]
33. Comuzzi, L.; Ceddia, M.; Di Pietro, N.; Inchingolo, F.; Inchingolo, A.M.; Romasco, T.; Tumedei, M.; Specchiulli, A.; Piattelli, A.; Trentadue, B. Crestal and Subcrestal Placement of Morse Cone Implant-Abutment Connection Implants: An In Vitro Finite Element Analysis (FEA) Study. *Biomedicines* **2023**, *11*, 3077. [CrossRef]
34. *ASTM F-1839-08*; Standard Specification for Rigid Polyurethane Foam for Use as a Standard Material for Test Orthopedic Devices for Instruments. American Society for Testing and Materials (ASTM): West Conshohocken, PA, USA, 2008.
35. Misch, C.E. Bone classification, training keys to implant success. *Dent. Today* **1989**, *8*, 39–44. [PubMed]
36. Misch, C.E. Bone density: A key determinant for treatment planning. In *Contemporary Implant Dentistry*, 3rd ed.; Mosby: St. Louis, MO, USA, 2007; pp. 130–146.
37. Do Vale Souza, J.P.; de Moraes Melo Neto, C.L.; Piacenza, L.T.; Freitas da Silva, E.V.; de Melo Moreno, A.L.; Penitente, P.A.; Brunetto, J.L.; Dos Santos, D.M.; Goiato, M.C. Relation Between Insertion Torque and Implant Stability Quotient: A Clinical Study. *Eur. J. Dent.* **2021**, *15*, 618–623. [CrossRef]
38. Mello, B.F.; De Carvalho Formiga, M.; Bianchini, M.A.; Borges, I., Jr.; Coura, G.; Tumedei, M.; Fuller, R.; Petrini, M.; Romasco, T.; Vaz, P.; et al. Insertion Torque (IT) and Implant Stability Quotient (ISQ) Assessment in Dental Implants with and without Healing Chambers: A Polyurethane In Vitro Study. *Appl. Sci.* **2023**, *13*, 10215. [CrossRef]
39. Comuzzi, L.; Tumedei, M.; Di Pietro, N.; Romasco, T.; Heydari Sheikh Hossein, H.; Montesani, L.; Inchingolo, F.; Piattelli, A.; Covani, U. A Comparison of Conical and Cylindrical Implants Inserted in an In Vitro Post-Extraction Model Using Low-Density Polyurethane Foam Blocks. *Materials* **2023**, *16*, 5064. [CrossRef]
40. Comuzzi, L.; Tumedei, M.; Covani, U.; Romasco, T.; Petrini, M.; Montesani, L.; Piattelli, A.; Di Pietro, N. Primary Stability Assessment of Conical Implants in Under-Prepared Sites: An In Vitro Study in Low-Density Polyurethane Foams. *Appl. Sci.* **2023**, *13*, 6041. [CrossRef]
41. Romasco, T.; Pignatelli, P.; Tumedei, M.; Hossein, H.H.S.; Cipollina, A.; Piattelli, A.; Inchingolo, F.; Di Pietro, N. The influence of truncated-conical implant length on primary stability in maxillary and mandibular regions: An in vitro study using polyurethane blocks. *Clin. Oral Investig.* **2023**, *28*, 28. [CrossRef]
42. Greenstein, G.; Cavallaro, J. Implant Insertion Torque: Its Role in Achieving Primary Stability of Restorable Dental Implants. *Compend. Contin. Educ. Dent.* **2017**, *38*, 88–95; quiz 96.
43. Oliveira, M.R.; Gonçalves, A.; Gabrielli, M.A.C.; de Andrade, C.R.; Scardueli, C.R.; Filho, V.A.P. The correlation of different methods for the assessment of bone quality in vivo: An observational study. *Int. J. Oral. Maxillofac. Surg.* **2022**, *51*, 388–397. [CrossRef] [PubMed]
44. Simeone, S.G.; Rios, M.; Simonpietri, J. "Reverse torque of 30 Ncm applied to dental implants as test for osseointegration"-a human observational study. *Int. J. Implant Dent.* **2016**, *2*, 26. [CrossRef]
45. Sennerby, L.; Meredith, N. Resonance frequency analysis: Measuring implant stability and osseointegration. *Compend. Contin. Educ. Dent.* **1998**, *19*, 493–498, 500, 502; quiz 504. [PubMed]
46. Macedo, J.P.; Pereira, J.; Vahey, B.R.; Henriques, B.; Benfatti, C.A.M.; Magini, R.S.; López-López, J.; Souza, J.C.M. Morse taper dental implants and platform switching: The new paradigm in oral implantology. *Eur. J. Dent.* **2016**, *10*, 148–154. [CrossRef]
47. Mishra, S.K.; Chowdhary, R.; Kumari, S. Microleakage at the Different Implant Abutment Interface: A Systematic Review. *J. Clin. Diagn. Res.* **2017**, *11*, ZE10–ZE15. [CrossRef]
48. Sennerby, L.; Meredith, N. Implant stability measurements using resonance frequency analysis: Biological and biomechanical aspects and clinical implications. *Periodontol. 2000* **2008**, *47*, 51–66. [CrossRef] [PubMed]
49. Romanos, G.E.; Delgado-Ruiz, R.A.; Sacks, D.; Calvo-Guirado, J.L. Influence of the implant diameter and bone quality on the primary stability of porous tantalum trabecular metal dental implants: An in vitro biomechanical study. *Clin. Oral. Implants Res.* **2018**, *29*, 649–655. [CrossRef] [PubMed]
50. Marquezan, M.; Osório, A.; Sant'Anna, E.; Souza, M.M.; Maia, L. Does bone mineral density influence the primary stability of dental implants? A systematic review. *Clin. Oral Implants Res.* **2012**, *23*, 767–774. [CrossRef]
51. Herekar, M.; Sethi, M.; Ahmad, T.; Fernandes, A.S.; Patil, V.; Kulkarni, H. A correlation between bone (B), insertion torque (IT), and implant stability (S): BITS score. *J. Prosthet. Dent.* **2014**, *112*, 805–810. [CrossRef]
52. Di Stefano, D.A.; Arosio, P.; Capparè, P.; Barbon, S.; Gherlone, E.F. Stability of dental implants and thickness of cortical bone: Clinical research and future perspectives. A systematic review. *Materials* **2021**, *14*, 7183. [CrossRef]
53. Ottoni, J.M.; Oliveira, Z.F.; Mansini, R.; Cabral, A.M. Correlation between placement torque and survival of single-tooth implants. *Int. J. Oral Maxillofac. Implants* **2005**, *20*, 769–776. [PubMed]
54. Scarano, A.; Degidi, M.; Iezzi, G.; Petrone, G.; Piattelli, A. Correlation between implant stability quotient and bone-implant contact: A retrospective histological and histomorphometrical study of seven titanium implants retrieved from humans. *Clin. Implant Dent. Relat. Res.* **2006**, *8*, 218–222. [CrossRef] [PubMed]
55. Gehrke, S.A.; Pérez-Díaz, L.; Mazón, P.; De Aza, P.N. Biomechanical Effects of a New Macrogeometry Design of Dental Implants: An In Vitro Experimental Analysis. *J. Funct. Biomater.* **2019**, *10*, 47. [CrossRef] [PubMed]
56. Comuzzi, L.; Tumedei, M.; Di Pietro, N.; Romasco, T.; Montesani, L.; Piattelli, A.; Covani, U. Are Implant Threads Important for Implant Stability? An In Vitro Study Using Low-Density Polyurethane Sheets. *Eng* **2023**, *4*, 1167–1178. [CrossRef]

57. Barikani, H.; Rashtak, S.; Akbari, S.; Badri, S.; Daneshparvar, N.; Rokn, A. The effect of implant length and diameter on the primary stability in different bone types. *J. Dent.* **2013**, *10*, 449–455. [PubMed] [PubMed Central]
58. Jimbo, R.; Tovar, N.; Marin, C.; Teixeira, H.S.; Anchieta, R.B.; Silveira, L.M.; Janal, M.N.; Shibli, J.A.; Coelho, P.G. The impact of a modified cutting flute implant design on osseointegration. *Int. J. Oral Maxillofac. Surg.* **2014**, *43*, 883–888. [CrossRef] [PubMed]
59. Sciasci, P.; Casalle, N.; Vaz, L.G. Evaluation of primary stability in modified implants: Analysis by resonance frequency and insertion torque. *Clin. Implant Dent. Relat. Res.* **2018**, *20*, 274–279. [CrossRef] [PubMed]
60. Del Fabbro, M.; Testori, T.; Francetti, L.; Weinstein, R. Systematic review of survival rates for implants placed in the grafted maxillary sinus. *Int. J. Periodontics Restor. Dent.* **2004**, *24*, 565–577. [CrossRef] [PubMed]
61. Gehrke, S.A.; Scarano, A.; de Lima, J.H.C.; Bianchini, M.A.; Dedavid, B.A.; De Aza, P.N. Effects of the healing chambers in implant macrogeometry design in a low-density bone using conventional and undersized drilling. *J. Int. Soc. Prev. Community Dent.* **2021**, *11*, 437–447. [CrossRef] [PubMed]
62. Gehrke, S.A.; Dedavid, B.A.; Aramburú, J.S., Jr.; Pérez-Díaz, L.; Guirado, J.L.C.; Canales, P.M.; De Aza, P.N. Effect of different morphology of titanium surface on the bone healing in defects filled only with blood clot: A new animal study design. *BioMed Res. Int.* **2018**, *2018*, 4265474. [CrossRef] [PubMed]
63. Romasco, T.; De Bortoli, N., Jr.; De Bortoli, J.P.; Jayme, S.J.; Piattelli, A.; Di Pietro, N. Primary stability evaluation of different morse cone implants in low-density artificial bone blocks: A comparison between high-and low-speed drilling. *Heliyon* **2024**, *10*, e35225. [CrossRef]
64. Borges, F.L.; Dias, R.O.; Piattelli, A.; Onuma, T.; Gouveia Cardoso, L.A.; Salomão, M.; Scarano, A.; Ayub, E.; Shibli, J.A. Simultaneous sinus membrane elevation and dental implant placement without bone graft: A 6-month follow-up study. *J. Periodontol.* **2011**, *82*, 403–412. [CrossRef] [PubMed]
65. Calvert, K.L.; Trumble, K.P.; Webster, T.J.; Kirkpatrick, L.A. Characterization of commercial rigid polyurethane foams used as bone analogs for implant testing. *J. Mater. Sci. Mater. Med.* **2010**, *21*, 1453–1461. [CrossRef] [PubMed]
66. Nagaraja, S.; Palepu, V. Comparisons of anterior plate screw pullout strength between polyurethane foams and thoracolumbar cadaveric vertebrae. *J. Biomech. Eng.* **2016**, *138*, 104505. [CrossRef] [PubMed]
67. Huang, H.M.; Lee, S.Y.; Yeh, C.Y.; Lin, C.T. Resonance frequency assessment of dental implant stability with various bone qualities: A numerical approach. *Clin. Oral Implants Res.* **2002**, *13*, 65–74. [CrossRef] [PubMed]
68. Cipollina, A.; Ceddia, M.; Di Pietro, N.; Inchingolo, F.; Tumedei, M.; Romasco, T.; Piattelli, A.; Specchiulli, A.; Trentadue, B. Finite Element Analysis (FEA) of a Premaxillary Device: A New Type of Subperiosteal Implant to Treat Severe Atrophy of the Maxilla. *Biomimetics* **2023**, *8*, 336. [CrossRef]
69. Di Pietro, N.; Ceddia, M.; Romasco, T.; De Bortoli Junior, N.; Mello, B.F.; Tumedei, M.; Specchiulli, A.; Piattelli, A.; Trentadue, B. Finite Element Analysis (FEA) of the Stress and Strain Distribution in Cone-Morse Implant–Abutment Connection Implants Placed Equicrestally and Subcrestally. *Appl. Sci.* **2023**, *13*, 8147. [CrossRef]